Positioning and Simulation of Human Body Models on a Motorcycle with a Novel Restraint System

Steffen Maier, Fabian Kempter, Stefan Kronwitter, Jörg Fehr

Abstract The objective of this research is to investigate the behaviour of motorcyclists in motorcycle to car impacts applying a novel safety restraint concept with state-of-the-art human body models (HBMs). A selection of current finite element HBMs with sex variants were positioned on the motorcycle's seat, footrests, and handlebar. Kinematics and kinetics of motorcyclists were simulated using HBMs and models of anthropomorphic test devices (ATDs) in representative impact scenarios. The scenarios were implemented with a finite element model representing motorcycle surfaces in interaction with the rider combined with vehicle impact trajectories derived from multi-body simulations.

The HBMs provided insight into kinematics and kinetics of motorcycle riders that cannot be identified by ATDs in a specific load case with a novel passive safety system for a motorcycle. The accordance of Hybrid III ATD and HBM simulation results was higher in the frontal impact configuration. The higher spine flexibility in the HBMs leads to later head-airbag impact times and greater head accelerations in the lateral crash configuration. Although variations in the HBM and ATD responses were observed, the proposed motorcycle's passive safety concept responded robustly to variations of the rider surrogates in all shown cases by preventing direct impacts on opposing vehicle structures.

Keywords Motorcycle Safety, Human Body Models, Finite Element Simulations, Passive Safety, Vulnerable Road Users.

I. INTRODUCTION

Powered two-wheelers have been gaining in popularity in Europe for several years. Despite the influences of the pandemic, annual new registrations of motorcycles and mopeds in Europe in 2021 surpassed pre-pandemic levels [1]. In western industrialised countries, motorcycles are often used as leisure vehicles. However, the motorcycle also offers practical advantages over conventional passenger cars. For example, in increasingly dense urban traffic, it is a manoeuvrable means of transportation that requires only a small parking area due to its compactness. The purchase and maintenance costs are also significantly lower. Using a motorcycle instead of a car is more environmentally sustainable because production and operation are more resource-efficient. According to [2], the average occupancy rate is only about 1.7 persons per car in EU countries. Since here the majority of trips (59%) are still made by car, this offers enormous potential for savings in terms of CO_2 emissions. However, these advantages are countered by the fact that motorcyclists are almost unprotected in the event of an accident, except for their personally worn riding gear. The dangerous nature of motorcycling is reflected in the accident statistics, e.g. Germany's [3]. In terms of 100,000 registered motorcycles, eleven motorcyclists were fatally injured in 2020, while only two vehicle occupants were killed per 100,000 passenger cars. Passenger cars are most frequently involved in fatal accidents involving motorcycle occupants. In collisions of this type, 94% of the fatally injured accident victims were motorcycle riders, although 68% of these accidents were caused by car drivers.

ATDs are designed to mimic human impact responses, such as kinematics and deformation, under high external loads based on experiments with post mortem human subjects (PMHS). However, ATDs are not omnidirectional applicable. Instead, there are specific ATDs, e.g. for different load directions and seating positions of car accident configurations. However, digital only, finite element (FE) human body models (HBMs), e.g. [4-5], can compensate for the shortcomings of ATDs and their numeric models and provide further insights. In these models, the musculoskeletal system of the human body is simulated as realistically as possible in terms of

S. Maier (e-mail: steffen.maier@itm.uni-stuttgart.de; tel: +49 711 685-66956) and F. Kempter are research associates and doctoral students, S. Kronwitter was a student, and J. Fehr is Professor, all at the Institute of Engineering and Computational Mechanics (ITM) at the University of Stuttgart, Germany.

geometry and material properties to be able to approximate the kinematics of a human being. This means that, unlike ATDs, HBMs are designed for omnidirectional use. For example, they have greater freedom of movement in the upper body due to the detailed modelling of the spine. Furthermore, depending on the level of detail, bone fractures or injuries in the muscles and organs may be predicted based on stresses and strains on tissue level [6]. However, the now very detailed and finely discretised modelling of HBMs also means that computation times can be many times higher than for models of ATDs. Compared to ATDs, which can be positioned by adjusting joint angles and applying nodal displacements based on these kinematic constraints, HBMs have complex joints and motion patterns with non-idealised degrees of freedom surrounded by deformable tissue, and positioning them is therefore difficult and laborious [7].

The objective is to use current state-of-the-art FE HBMs to represent motorcyclists in accidents. The novelty of this study is a detailed description of a simulation-based approach to position HBMs onto a motorcycle. Currently, FE HBMs are very rarely used to represent riders of motorcycles or other powered two-wheelers in accident simulations. In [8], a helmeted 50th percentile male THUMS HBM was used to simulate the influence of helmet design in primary impacts against a car and ground impacts. In [9], a 50th percentile THUMS was used to represent riders of an electric scooter and a bicycle in collisions with cars. In [10-11] the impact behaviour of a 5th percentile THUMS as the rider of a small motorcycle and a six-year old THUMS variant as a pillion passenger against a passenger car and a pickup truck have been investigated. A description of the procedure for the positioning and discussion of the resulting postures of the models was not part of these works. Furthermore, no comparison of multiple HBMs or between female and male riders is made. In this study shown here, the robustness of the positioning approach and the safety systems is shown to multiple HBMs including sex variants.

This leads to the research questions that are addressed in this paper. RQ1: Are current virtual HBMs also suitable for being positioned on a motorcycle and representing motorcyclists in accidents? How do the responses of various HBMs vary, and how do they differ from accident simulations of ATDs? RQ2: What simulation methodologies can be used to evaluate this with sufficient numerical efficiency to deal with current HBM complexity? In this paper, this is investigated using the example of a novel safety concept for motorcycles, which restrains the motorcyclist on the motorcycle in the event of an accident, guides and controls their accident trajectory, and prevents them from hard impacts against an accident opponent. One specific methodological-technical novelty of this study is a systematic approach to the positioning of complex state-of-the-art HBMs in the posture of a motorcyclist on a motorcycle, which has not been established before, and its discussion. An application of the shown procedures for several HBMs and sex variants is performed and a comparison of their behaviour in motorcycle accidents with a novel safety system is shown.

II. METHODS

Motorcycle Model with Novel Restraint Safety Concept

A novel safety concept for a motorcycle, shown in Fig. 1, envisages restraining the rider on the motorcycle in the event of an accident, guiding their accident trajectory, and preventing them from being subjected to hard impacts. It consists of thigh seat-belts, multiple airbags, foam leg impact protectors, and a newly designed motorcycle body surrounding the lower extremities as a side-impact structure. The bodywork, together with two side airbags, two mirror airbags and a frontal airbag, forms a protective envelope around the rider and is thus intended to prevent a hard impact to the head and upper body in the initial accident phase. These measures are intended to provide the occupant with sufficient protection so that it is not necessary to wear a helmet.

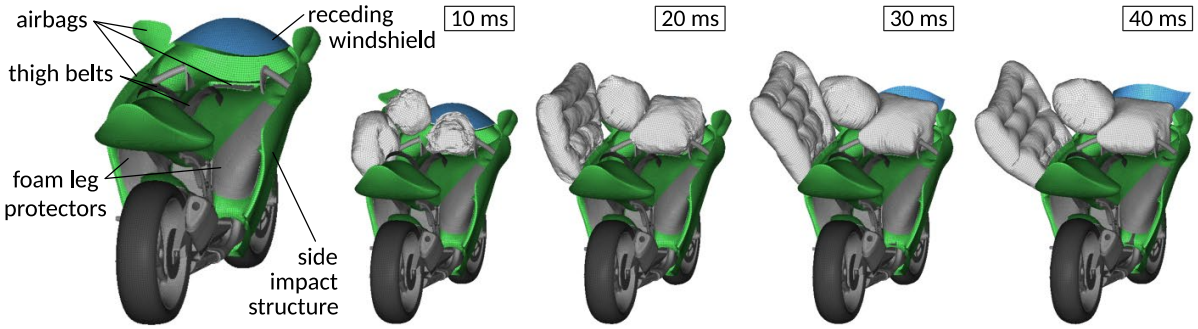

Fig. 1. Safety systems of the novel safety concept for motorcycles as a full FE representation and inflation process of the airbags, representing the left half of the concept's airbag protection.

Simulation Strategy with MB-Trajectories of Motorcycle and Accident Opponent in a FE Environment

The strategies commonly used in current automotive development for occupant protection break down the accident event into several individual problems. For example, in experiments and simulations, the interaction of the vehicle with an accident opponent and the behaviour of its occupants inside the vehicle are mostly considered separately. In [12], we provided a simulation strategy with an equivalent approach for the given motorcycle and restraint system. It consists of multiple successive virtual development stages with a continuously increasing level of detail. As part of this strategy, Fig. 2 (left) shows the multi-body (MB) model of the motorcycle, the airbags, the belts, a rider surrogate, and the accident opponent in a MB approach in the simulation environment MADYMO presented in [13]. This model is based on simulations of full-scale crash tests of conventional motorcycles against passenger cars fitted to experimental results. After the initial airbag and seat-belt concept simulations, the next step is to perform FE simulations. Figure 2 (right) shows a model representing the motorcycle cockpit in more detail in the FE software environment LS-DYNA, with deformable cockpit surfaces and including foam impact protection [14-15]. To reproduce the impact dynamics, the multiaxial rigid body motions of the MB simulations are applied as prescribed motions for the outer bodies of motorcycle and car at their centre of gravity (COG), with the car body geometry acting only as a reaction surface for the airbags. As seen in Fig. 2 (right) the rider is now represented by an HBM. Similar to simulations of sled tests of a car interior, this simulation setup is very well suited to study human accident response in a reproducible manner while also significantly reducing computation costs compared to a full FE model representation with fully deformable motorcycle and car structures.

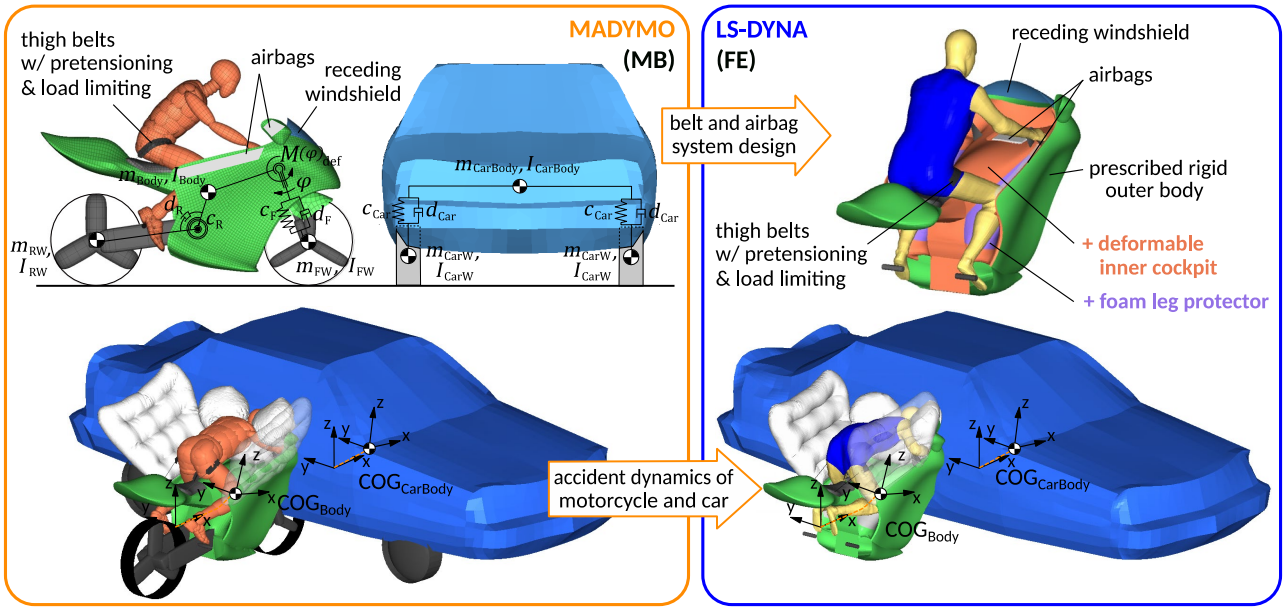

Fig. 2. MBS and FE simulation strategy and LS-DYNA MB trajectory implementation from MADYMO.

HBMs as Male and Female Motorcycle Rider Surrogates

Three current state-of-the-art FE HBMs (GHBMC [16], THUMS [17], and ViVA+ [18-20]) and sex variants (female and male ViVA+) with varying levels of detailing and degrees of freedom were selected, see Fig. 3 (a)–(d). Each of the male versions is intended to represent a 50th percentile male, and the female model to represent a 50th percentile female human.

The overall posture of a motorcycle rider depends on their anthropometric body dimensions and the geometry of the motorcycle. As shown in Fig. 4, in principle, the posture must fulfil four boundary conditions: (i) the pelvis is on the seat (equates to a surface contact), while its absolute position can be varied to a limited extent; (ii) the hands grip the handles of the handlebar (revolute joint); (iii) the feet are positioned on the footrests (revolute joint); and (iv) the head must comply with a visual condition which typically results in a downward orientation of the head of about 10–15° to the horizontal (orientation constraint). The resulting posture is unstable and must be maintained by static muscle power. To define the target posture for the investigated human models, experimentally determined posture data from [21] was used as a guide. In this study, the postures of several test subjects were examined for different types of motorcycles in a wind tunnel at a frontal velocity of 120 km/h. The chosen posture angles in the work presented here are given in Table I, which correspond to a typical posture of a rider on a sports bike in [21].

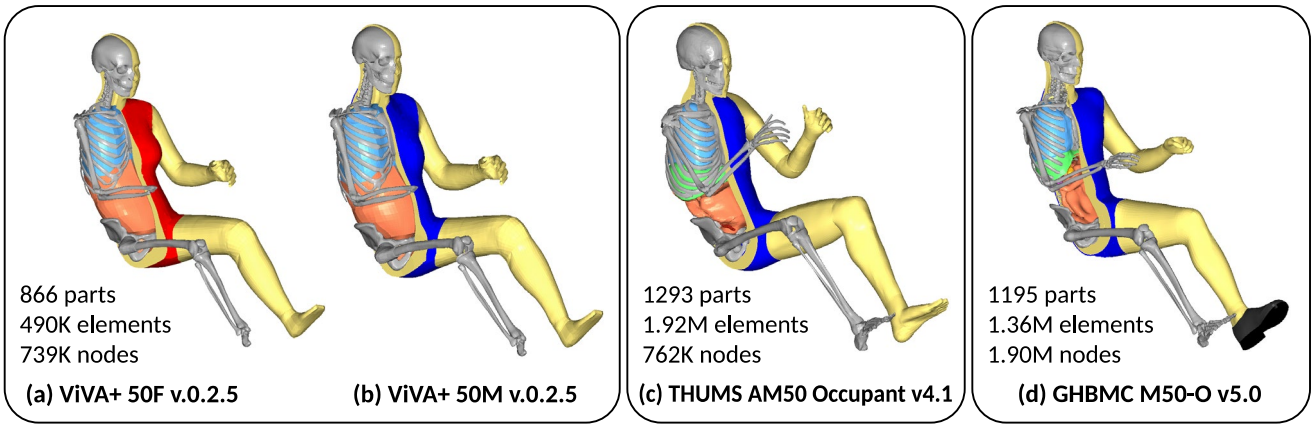

Fig. 3. Overview of this study's female and male state-of-the-art HBMs in their default seating position, mainly intended to represent postures of a passenger car occupant.

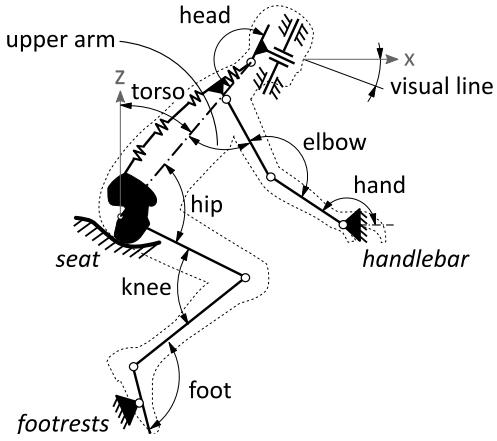

Fig. 4. Principle framework to describe the posture of a motorcycle rider with angle definitions according to [21].

TABLE I
POSTURE ANGLES OF SEATED MOTORCYCLE RIDER ACCORDING TO CONVENTION IN FIG. 4

visual line	15°
head	165°
upper arm	70°
elbow	150°
hand	150°
torso	40°
hip	75°
knee	65°
foot	115°

The positioning of the selected complex FE models in the body postures of motorcyclists in interaction with a motorcycle presents challenges and is a laborious task. The default positions of the models are either standing postures for pedestrians or postures of passenger car occupants, as shown in Fig. 3. A multi-stage simulation-based process was devised to achieve the posture of a motorcyclist, which is illustrated in Fig. 5 using the ViVA+ 50M as an example.

In a first step (1) the HBM was pre-positioned in the motorcyclist's body posture. The open-source tool PIPER [22] was used to define a transient pre-positioning simulation that prescribes the motion of the skeletal structure via elastic elements. Here, the joint angles of the lower and upper extremities were altered, defining joint angles and landmark positions interactively. As positioning target, reference surfaces of the motorcycle cockpit, footrests and grips oriented in respect to the default HBM orientation were loaded into the PIPER software interface. The spine shape remained unchanged as the PIPER functionalities didn't show stable behaviour for the investigated HBMs and application cases. Finally, the motion sequence curves for a transient LS-DYNA simulation were exported from PIPER.

In step (2) the HBM was seated into the seat and motorcycle cockpit. The contact surfaces of the motorcycle, the seat, the handles, the footrests, and the other cockpit surfaces (shown in red) were initially scaled and distorted. During the seating and contact initialisation simulation, these geometries were morphed into the motorcycle's actual geometry. This was used to rotate the HBM's wrists and initialise contacts with the motorcycle surfaces. Contact initialisation means that contacts were defined between the HBM and the motorcycle parts and the HBM segments made contact with the corresponding motorcycle components. To keep the HBM upright, gravity was not applied during step (1) and (2). To keep the HBM attached to the motorcycle and to push it into the seat, the pelvis and feet were elastically restrained with spring elements fixed to space (shown in green). To raise the head, a spring element connected to the skull was translated by a prescribed node (shown in magenta).

The final step (3) is the actual crash simulation. It starts immediately before the impact, with an initial velocity. The subsequent impact dynamics are imposed motions with linear acceleration and angular velocity time histories of the rigid bodies in the MB environment, as outlined in Fig. 2.

For quick positioning and achieving short simulation durations, global damping of the model was applied in steps (1) and (2). No gravity loading was considered during steps (1) and (2); it was adopted only during step (3). In this multi-step procedure, the posture pre-positioning (1), the seating and contact initialisation (2), and actual crash (3) are separate simulations in between which the nodal coordinates of the FE mesh are exchanged via MATLAB procedures. However, all other information from the respective previous simulations is not considered in the crash simulation, e.g. stresses and strains in the elements or geometry-dependent model parameters.

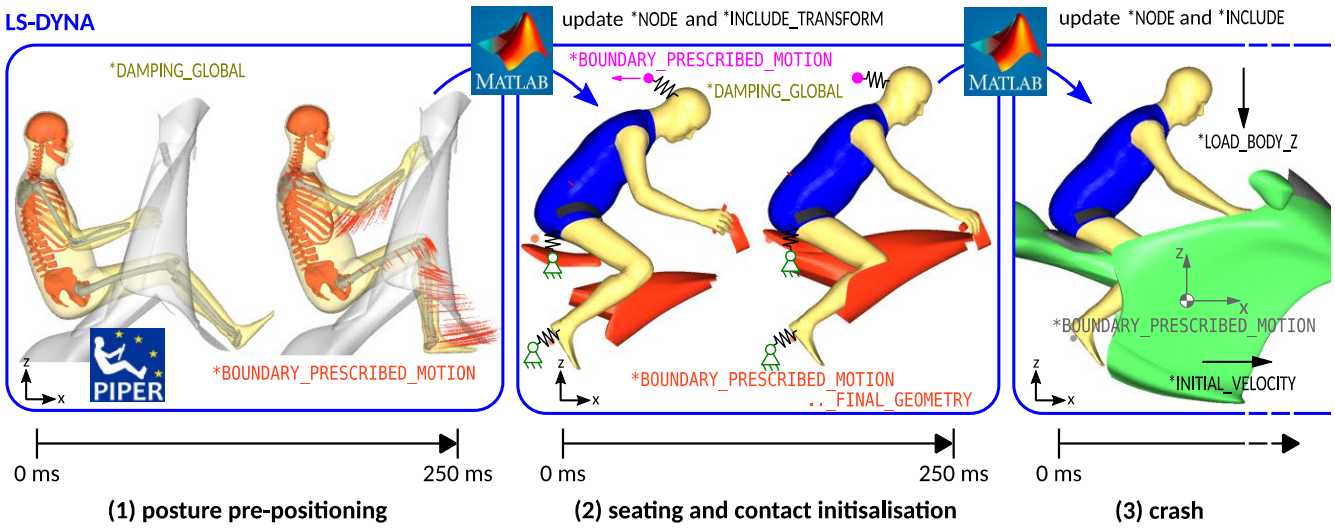

Fig. 5. Multi-step HBM positioning and procedure with multiple individual simulations for posture pre-positioning, seating and contact initialisation, and impact simulation with the most important LS-DYNA keywords.

To position humans of different heights on the motorcycle, an adjustable handlebar and adjustable footrests were considered, which are available for motorcycles. For the female HBM the handles were placed 75 mm backwards; the footrests were placed 50 mm forwards and 40 mm upwards. In Fig. 6 (a)–(d) the resulting HBM riding postures are shown. The coloured overlay in Fig. 7 shows that, despite anthropometric differences, the resulting postures of the male surrogates are overall very similar. Only the position and angle of the elbows visibly differ significantly from each other. Another difference between the models is the result of the modelling of the hands. The ViVA+ and GHBMC hands are modelled as rigid bodies and are therefore not deformable, which means that the fingers pierce the handles, which are also rigid (as with the ViVA+ hand), or thinner handles must be specially formed (as with the GHBMC hand). Only THUMS allows realistic gripping of the handles due to the deformable modelling of the hands.

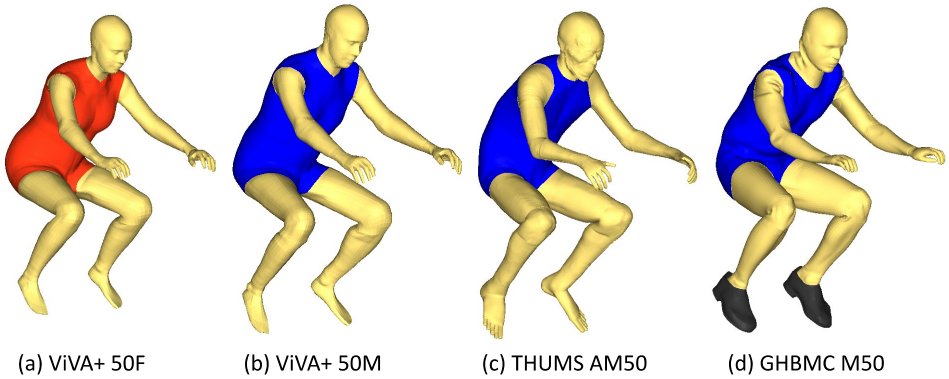

Fig. 6. Positioned and seated HBMs in the motorcyclist's riding postures achieved at the end of step (2).

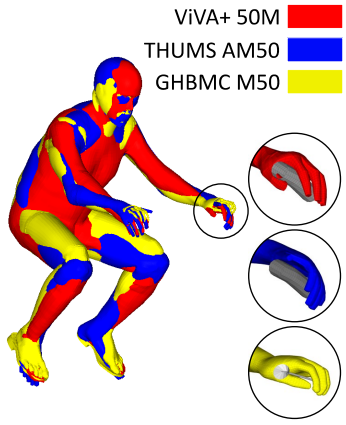

Fig. 7. Overlay comparison of the resulting postures of the male surrogate models.

ATDs as Male and Female Motorcycle Rider Surrogates

For the investigation of motorcycle accidents, the Motorcyclist Anthropometric Test Device (MATD) [23], specified by ISO 13232-4 [24], was developed, which is based on the pedestrian version of the Hybrid III 50th percentile man. Some modifications were made to the Hybrid III ATD for a more realistic representation of a motorcyclist. The MATD: (i) features more range of motion in the hips and torso, which improves positioning on a motorcycle; (ii) has an increased range of motion and more realistic torsional stiffness in the neck; (iii) the upper body is more compliant; (iv) it can wear a helmet; and (v) it can clasp the handlebar grips with its hands. This ATD is very expensive, however, and is therefore rarely used in crash tests. Despite the recommendation of ISO 13232 [24] to use the MATD, numerical models (LSTC Detailed release 190217) of the Hybrid III 50th percentile (average male) and III 5th percentile (small female) frontal impact ATD were used in this study. This selection was justified because: (i) helmet compatibility is not a requirement since no helmet is worn; (ii) the Hybrid III was also used in the simulation models of full-scale crash tests to fit the multi-body vehicle models; (iii) we want to assess a diverse group of riders and there is only an average male MATD available; and, most significantly, (iv) the sit/stand pelvis of the MATD has deep clefts between the flesh components at the hip joints, which are not compatible for attaching the thigh belts. The positioning of the ATDs corresponds to the procedure and their final postures already presented in a previous work [14].

Accident Configurations

The International Standard ISO 13232-2:2005 [24] recommends very frequent accident configurations, which are recommended based on 501 real motorcycle-to-car accidents in Hannover (Germany) and Los Angeles (USA). In each of the seven recommended configurations, shown in Fig. 8, the motorcycle collides with a passenger car in an initial upright motorcycle position. The nomenclature XXX – YY/ZZ is identified by a three-digit code, XXX, representing the relative geometric positions of the motorcycle and the opposing vehicle, followed by the impact speeds in meters per second of the opponent vehicle YY and motorcycle ZZ. Concordant to ISO 13232 the opposing passenger car was represented by a 1987 Ford Scorpio, a four-door saloon with a mass of 1,410 kg and an overall height of 141 cm.

In this study, it was aimed to investigate frontal and lateral loading of the riders. For this, impact configurations ① and ⑦ are considered. Because of a relative motion of the opposing vehicles in ②-⑥, these result in an oblique loading of the rider. In the selected two accident scenarios ① and ⑦, the accident trajectory of the rider is largely in a single plane. For ① it is in the x-y-plane of the motorcycle, see, e.g., Fig. 10 and for ⑦ it is in the x-z-plane of the motorcycle, see, e.g., Fig. 9. This allows a good comparison of the trajectories of each body region of the rider in the selected impact configurations with an isolated investigation of frontal and lateral response of the riders. In impact configuration ① the stationary motorcycle is hit laterally by the passenger car, which is travelling at 35 km/h at a relative angle of 90°. In configuration ⑦, the motorcycle impacts head-on at 48 km/h at a right-angle into the side of the stationary car right at its centreline.

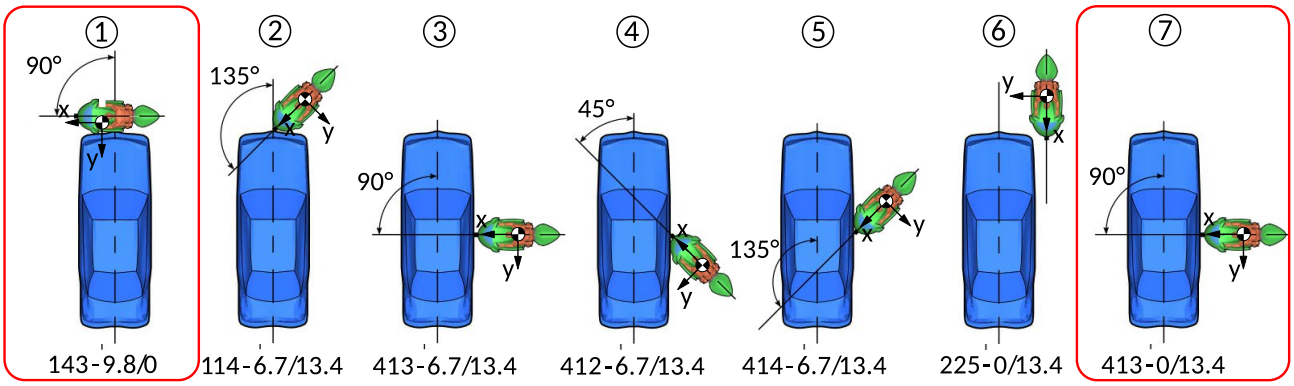

Fig. 8. Accident configurations of a motorcycle and a passenger car according to ISO 13232:2005. Configurations used in this investigation are outlined in red.

III. RESULTS

Impact Response of ATDs and HBMs

First, the impact kinematics of ATDs and HBMs were compared. In Fig. 9 and Fig. 10 the resulting motion during the primary impact, the immediate period after contact of the two vehicles, for the Hybrid III 50th percentile ATD and the ViVA+ 50M HBM is shown. For this purpose, the models were partially displayed transparently to illustrate the mechanical or human skeletal structure. In configuration ⑦ (Fig. 9), a frontal collision of the motorcycle against a stationary car, the rider was restrained by the thigh belts. The frontal airbag decelerated the resulting upper-body rotation. The comparison shows very similar upper-body motions, while the moulded flesh in the pelvic region of the ATD kept the thighs perpendicular to the upper body, unlike the HBM. In configuration ① (Fig. 10), where the stationary motorcycle was hit laterally by the car, the side airbag deployed within ~35 ms to the side of the rider and afterwards was pushed down by the rider's lateral rotational motion and cushioned the rider's impact. Here, clear differences in the motion sequence of the upper bodies became apparent. The spine of the HBM was laterally more flexible than the mechanical replication of that of the ATD. This is shown at 75 ms by a delayed motion of the head and at 150 ms by a more consistently deflected spine, including the neck. In addition, a greater deformation in the torso of the HBM can be observed.

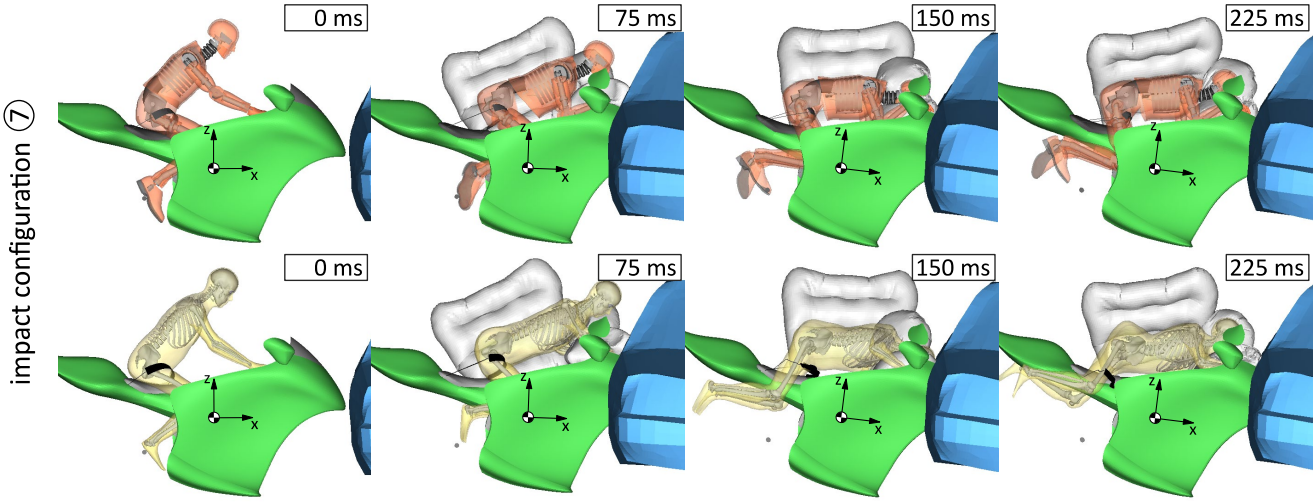

Fig. 9. Comparison of ATD (top: 50th percentile Hybrid III) and HBM (bottom: ViVA+ 50M) kinematic impact responses in configuration ISO-13232 configuration ⑦.

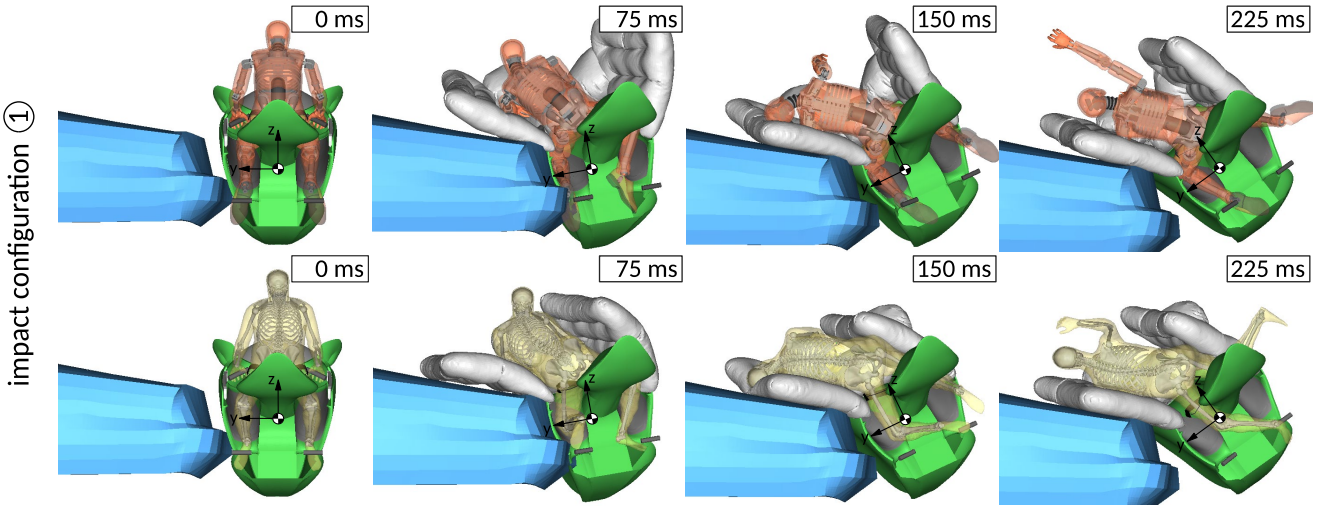

Fig. 10. Comparison of ATD (top: 50th percentile Hybrid III) and HBM (bottom: ViVA+ 50M) kinematic Impact responses in configuration ISO-13232 configuration ①.

In Fig. 11 and Fig. 12 a comparison of the sex variants of ViVA+ is made. Here, the skeletal structure of the head COG (red), the cervical (blue), thoracic (green), and lumbar spine (orange) as well as upper (brown) and lower (grey) extremities was overlaid. The trajectories of the head COG, C7, T12, and L5 were tracked relative to the motorcycle COGs. For configurations ⑦ and ① motions are nearly identical. Only when rebounding from the front airbag in ⑦, the female HBM appeared to have received more recoil with the head in both cases. This shows that the current airbag design, which is determined by the geometry of the airbag, the mass inflow parameters and the exhaust area, is sensitive to the mass of the rider.

The ViVA+ provides a default output for head COG node history based on an interpolated node set constraint. A comparison with the Hybrid III 5th and 50th head COG sensor linear and angular accelerations is given in Fig. 13. The head injury criteria HIC(36 ms), a_{3ms}, GAMBIT, and BriC(CMSD) based on linear acceleration a, angular acceleration $\ddot{\varphi}$, and angular velocity ω were calculated. Their determination and respective biomechanical limits are given Appendix A. The linear accelerations and the derived HIC(36 ms) and a_{3ms} injury criteria show that the resulting accelerations are very similar for configuration ⑦. For configuration ① they are significantly higher for the HBMs and occur later (~0.125 s vs.~0.09 s), see Fig. 15 on the top right. It appears that the later response of the head, due to a less stiff spine and neck, results in significantly greater acceleration values. The angular accelerations and the injury criteria that also rate head rotations, GAMBIT and BrIC, are for the HBMs also higher compared to those of the ATDs. As shown in the table data of Fig. 13, the BrIC values are very often above the recommended limit. This criteria evaluates maximal values of the angular velocity components $\omega_{x/y/z}$ to critical angular velocities $\omega_{xC/yC/zC}$, here based on a Cumulative Strain Damage Measure (CSDM), where a value of 1 corresponds to a 50% probability of AIS4+ brain injuries [25].

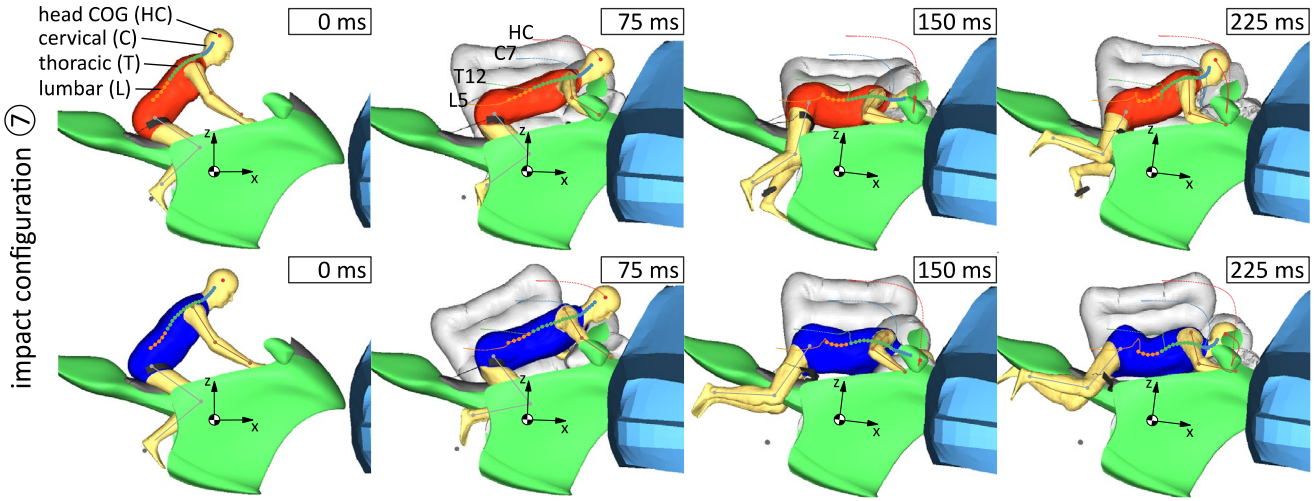

Fig. 11. Impact simulations of ViVA+ 50F (top) and ViVA+50M (bottom) according to ISO-13232 configuration ⑦ with skeletal trajectories relative to the motorcycle's centre of gravity. Note that in ⑦ only the right arm and leg skeletal trajectories are shown.

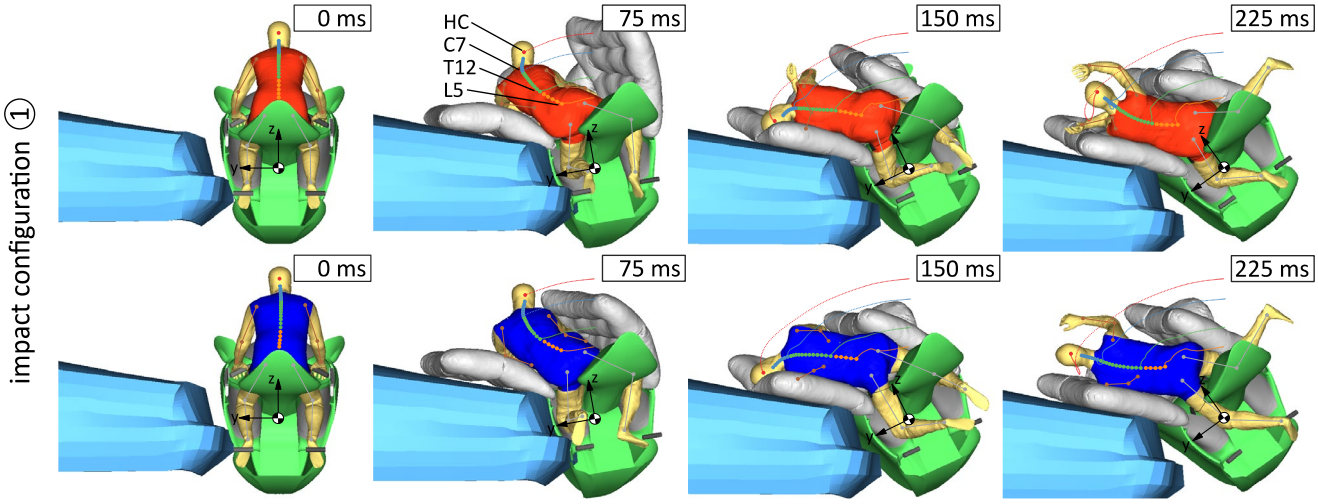

Fig. 12. Impact simulations of ViVA+ 50F (top) and ViVA+ 50M (bottom) according to ISO-13232 configuration ① with skeletal trajectories relative to the motorcycle's centre of gravity.

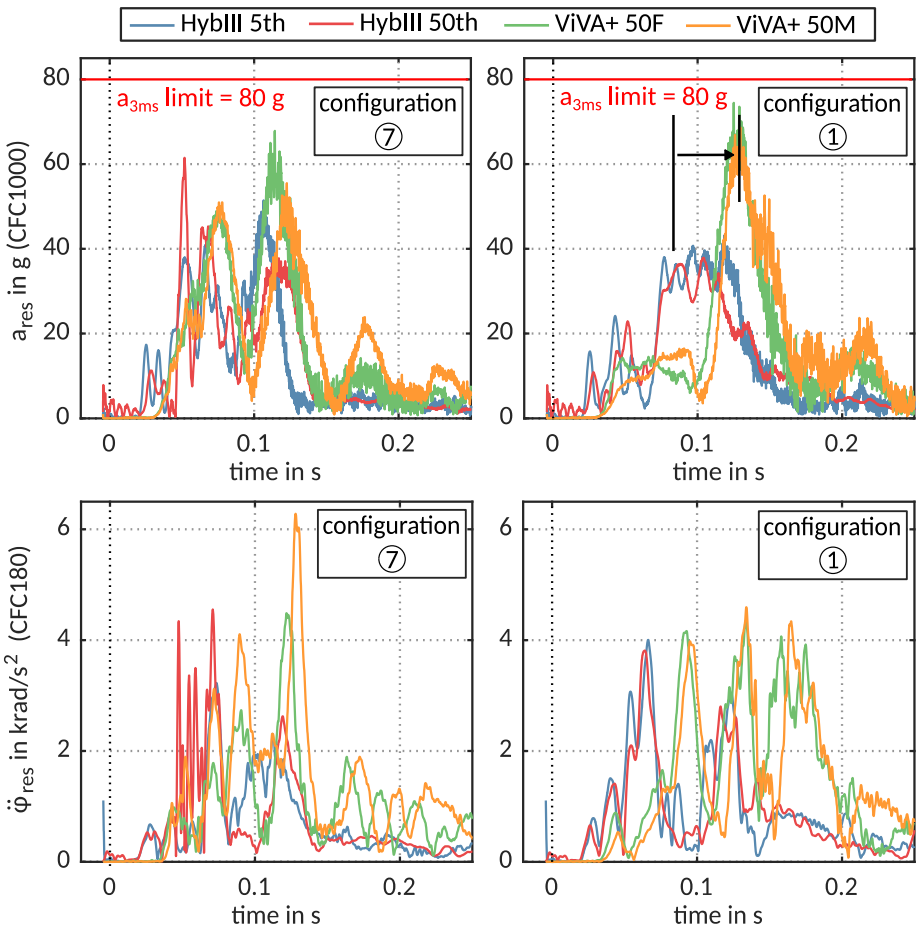

injury criteria	HIC(36)/a_{3ms}			
configuration	⑦		①	
HybIII 5th	213	43 g	280	38 g
HybIII 50th	207	51 g	226	37 g
ViVA+ 50F	429	52 g	676	64 g
ViVA+ 50M	286	46 g	626	58 g

injury criteria	GAMBIT/BrIC			
configuration	⑦		①	
HybIII 5th	0.22	0.65	0.23	1.01
HybIII 50th	0.29	0.51	0.23	1.01
ViVA+ 50F	0.31	0.70	0.34	1.57
ViVA+ 50M	0.36	1.01	0.33	1.38

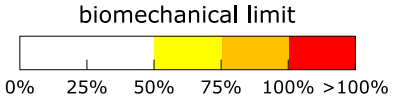

Fig. 13. Resulting head COG linear (top) and angular (bottom) accelerations for ATDs and ViVA+ HBMs with head injury criteria for configuration ⑦ (left) and ① (right). The table data are colour-coded for severity of the head injury criteria in respect to the biomechanical limits from [25]. See Appendix A for calculation of the injury criteria.

Comparison of Impact Response for Selected HBMs

Figure 14 shows an overview of the impact time history for the selected male HBMs based on their skeletal structure. For each of the snapshots, the main skeleton structure was overlayed and the trajectories of head COG, C7, T12, and L5 were traced. The positions were obtained by predefined default landmarks of the HBMs which were selected to be equivalent. Note that the THUMS simulation of configuration ① failed at 163 ms, because of failing brain elements that could not be prevented, although the troubleshooting guidelines provided were applied. The individual animations of the summarised simulations of THUMS and GHBMC are provided in Appendix B. The given trajectories show minor variations in the initial position of the skeletal structures and mainly the same impact response for the HBMs upon impacting the airbags. In comparison, the ViVA+ slipped the furthest out of the thigh belts in ①. This did not cause it to move out of range of the side airbag and thus miss the airbag, but it could be problematic in the subsequent secondary impact phase. The GHBMC model behaved stiffer in the upper body compared to the ViVA+ and THUMS models, resulting in more neck deflection in ①.

For the given vehicle impact dynamics, the safety concept of the motorcycle unfolded its proposed effect in all shown cases. The HBMs were effectively restrained to the motorcycle by the thigh belts for the primary impact. The surrounding airbags decelerated the resulting frontal or lateral upper-body rotation about the fixed pelvis and prevented the head and torso contact to motorcycle and car. Figure 15 gives the corresponding resultant linear and angular acceleration of the head COG and the derived head injury criteria for ViVA+ 50M and GHMBC; THUMS does not provide an output for head accelerations. The linear accelerations show a similar qualitative course, with the time histories and injury criteria of HIC(36) and a_{3ms} of the GHBMC quantitatively between ViVA+ 50M and Hybrid III 50th percentile. The same applies to the angular accelerations and the BrIC criterion associated with it. Here, the values of GHBMC are significantly lower than those of ViVA+. A breakdown of the rotation components based on the rotation velocities as well as the determination of the BrIC criterion for the cases presented here are attached in the Appendix C.

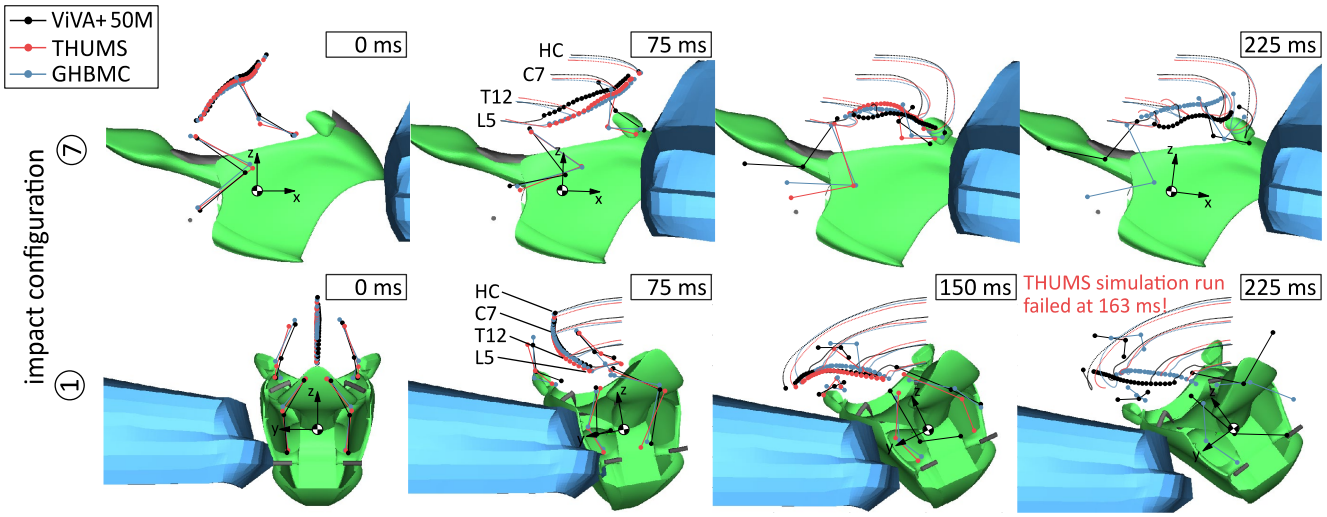

Fig. 14. Skeletal trajectories of the male HBM variants, ViVA+ 50M, THUMS and GHBMC, relative to the motorcycle's centre of gravity according to ISO-13232 configuration ⑦ (top) and ① (bottom). Note that in ⑦ only the right arm and leg skeletal trajectories are shown.

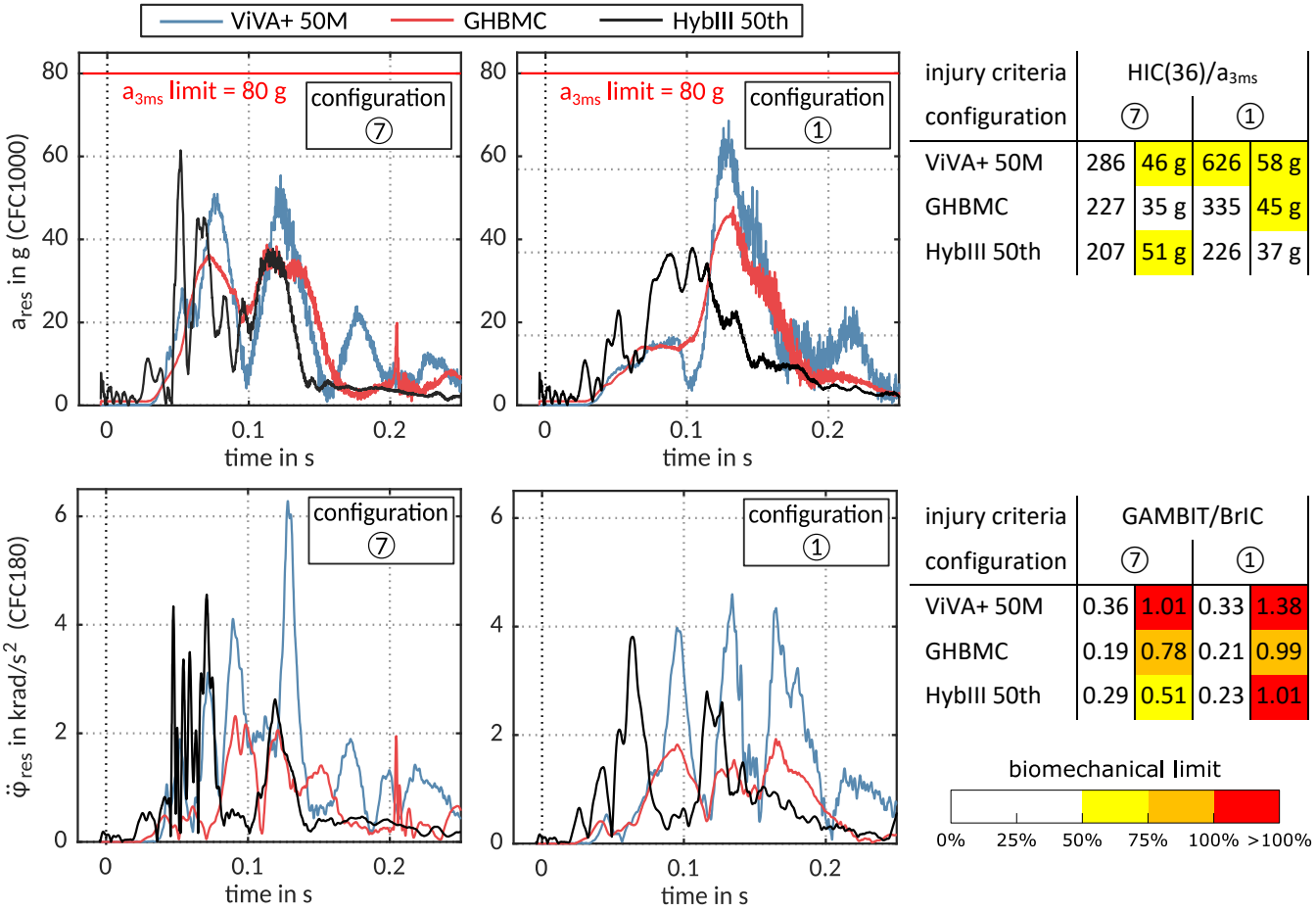

injury criteria	HIC(36)/a_{3ms}			
configuration	⑦		①	
ViVA+ 50M	286	46 g	626	58 g
GHBMC	227	35 g	335	45 g
HybIII 50th	207	51 g	226	37 g

injury criteria	GAMBIT/BrIC			
configuration	⑦		①	
ViVA+ 50M	0.36	1.01	0.33	1.38
GHBMC	0.19	0.78	0.21	0.99
HybIII 50th	0.29	0.51	0.23	1.01

Fig. 15. Resulting head COG linear (top) and angular (bottom) accelerations for male HBM variants, ViVA+ 50M, GHBMC and Hybrid III 50th percentile, with head injury criteria for configuration ⑦ (left) and ① (right).

IV. DISCUSSION

The proposed positioning and seating method enabled the positioning of multiple current complex FE HBMs in characteristic body postures of a motorcyclist on a motorcycle. The resulting postures showed expected variations due to the anthropometric differences of the HBMs and ATDs used in this study. The positioning method is time-consuming and labour-intensive, and it is an iterative process to achieve the desired posture targets in interaction with the four boundary conditions, i.e. the seat, the footrests, the handlebar, and the rider's

visual line. The laborious process shows that methods are needed to further systematize, automate and improve the technique, e.g. by using stress initialization.

The work presents an interesting application of HBMs as an omnidirectional tool to assess human accident behaviour. The HBMs provided additional insight in predicting the impact response of real-world human behaviour that the selected ATD surrogate could not represent. The results from the different HBMs and sex variants exhibited some kinematic variations but did not fundamentally contradict each other. In the frontal configuration ⑦ the HBMs showed similar results to the Hybrid III ATD, while larger deviations were present in the lateral configuration ①. The higher head linear and angular acceleration values at later times in the HBM simulations of the lateral scenario ① can be explained by the higher spine flexibility in these models compared to the Hybrid III. Outside of its actual use case of frontal impacts, the performance of the Hybrid III ATD is supposed to be less accurate than that of the HBMs, which have better omnidirectional applicability. However, additional scenario-specific validations should be performed to solidify the biofidelity of the HBMs, i.e. their lateral spine flexibility, in this type of crash loading. Validations of HBMs, currently based mainly on standard lateral car crashes with a 3-point seat-belt, should be extended because the motorcycle rider shows larger head, torso, and thus spine displacements in configuration ① due to the less restrained posture.

The motorcycle's proposed passive safety concept responded robustly to variations of the HBMs in all investigated cases by preventing direct impacts on vehicle structures during the primary impact. However, the BrIC criterion, determined from angular velocities of the head, showed significant loading exceeding the recommended biomechanical limit. Also, the observed slipping of the belts in ① for one of the HBMs showed that behaviour in secondary accident phases must also be considered and investigated in the future. To better understand and evaluate the consequences of impacts to the whole body, many other injury criteria must be considered and evaluated. Numeric human models offer many possibilities that should be utilised in the future, i.e. with the methods presented in [26].

Studies on passive safety of motorcyclists are not on a par with passenger car crash safety, especially in crash simulation. New virtual methods are needed to simulate motorcycle accidents at different levels of detail and system complexity. Using a detailed FE motorcycle cockpit, with prescribed crash pulses as vehicle dynamics, allowed for a reproducible and numerically efficient setup to compare rider surrogates' accident responses. The strategy is very similar to common car occupant safety development strategies. With this strategy, the vehicle trajectories stay unaffected for different rider models and therefore do not consider potential effects of changed mass and inertia properties of the riders on the motorcycle. Since the motorcycle is much lighter in respect to the rider compared to typical car/occupant ratios, neglecting potential changes in the interaction forces applied from the rider to the motorcycle may be a limitation of the strategy.

V. CONCLUSIONS

The described simulation-based approach allowed the positioning of complex FE HBMs in the characteristic posture of a motorcyclist on a motorcycle. In the investigated motorcycle to car impacts with a safety concept using airbags and thigh belts, the detailed HBMs showed different behaviour compared to ATD models for lateral impact loading. The higher spine flexibility of the HBMs lead to changed timing and magnitude of maximal head acceleration. Injury criteria and their corresponding biomechanical limits rated rotational head loading evaluated by rotational velocities as the most critical.

VI. ACKNOWLEDGEMENTS

We thank the VIRTUAL project consortium for providing access to their ViVA+ human models and the fruitful discussions in context of this research contribution.

VII. REFERENCES

[1] ACEM (2021) "ACEM statistical release 2021", https://www.acem.eu/images/publiq/2022/ACEM_-_Statistical_press_release_-_January_-_December_2021.pdf. [2022-05-05]

[2] Fiorello, D., Martino, A., Zani, L. and Christidis, P., Elena, N. (2016) Mobility Data across the EU 28 Member States: Results from an Extensive CAWI Survey, *Transportation Research Procedia*, 2016, **14**:pp.1104–1113.

[3] Statistisches Bundesamt (2021) Verkehrsunfälle: Kraftrad- und Fahrradunfälle im Straßenverkehr 2020. (in German)

[4] Iwamoto, M., Kisanuki, Y., *et al*. (2002) Development of a Finite Element Model of the Total Human Model for Safety (THUMS) and Application to Injury Reconstruction. *Proceedings of the IRCOBI Conference*, 2002, Munich, Germany.

[5] Östh, J., Mendoza-Vazquez, M., Linder, A., Svensson, M. Y., Brolin, K. (2017) The VIVA OpenHBM Finite Element 50th Percentile Female Occupant Model: Whole Body Model Development and Kinematic Validation. *Proceedings of the IRCOBI Conference*, 2017, Antwerp, Belgium.

[6] Forman, J. L., Kent, R. W. *et al.* (2012) Predicting Rib Fracture Risk with Whole-Body Finite Element Models: Development and Preliminary Evaluation of a Probabilistic Analytical Framework. *Annals of Advances in Automotive Medicine/Annual Scientific Conference*, 2012, Seattle, WA, USA.

[7] Klein, C., González-García, M. *et al.* (2021) A Method for Reproducible Landmark-based Positioning of Multibody and Finite Element Human Models. *Proceedings of IRCOBI Conference*, 2021, Munich, Germany.

[8] Kofler, D., Tomasch, E., Spitzer, P., Klug. C. (2020) Analysis of the Effect of Different Helmet Types and Conditions in Two Real-world Accident Scenarios with a Human Body Model. *Proceedings of IRCOBI Conference*, 2020, Munich, Germany.

[9] Huang Y, Zhou Q, Tang J, Nie B. (2018) A Preliminary Comparative Study on Rider Kinematics and Injury Mechanism in Car-to-Two-Wheelers Collisions. *Proceedings of IRCOBI Conference*, 2018, Athens, Greece.

[10] Carmai, J., Koetniyom, S., Hossain, W. (2020) Study of Motorcyclist's Injury Patterns in Motorcycle-Pickup truck Collision using Finite Element Simulations. *Proceedings of IRCOBI Asia Conference*, 2020, Bejing, China.

[11] Carmai, J., Koetniyom, S., Hossain, W. (2019) Analysis of Rider and Child Pillion Passenger Kinematics Along with Injury Mechanisms During Motorcycle Crash, Traffic Injury Prevention, 2019, **20**:pp.13–20.

[12] Maier, S., Fehr, J. (2021) Multi-Stage MBS and FE Simulation Strategy to Design a Safe Motorcycle (Extended Abstract). *Proceedings of ECCOMAS Thematic Conference on Multibody Dynamics*, 2021, Budapest, Hungary.

[13] Maier, S., Doléac, L., Hertneck, H., Stahlschmidt, S., Fehr, J. (2020) Evaluation of a Novel Passive Safety Concept for Motorcycles with Combined Multi-Body and Finite Element Simulations. *Proceedings of IRCOBI Conference*, 2020, Munich, Germany.

[14] Maier, S., Doléac, L., Hertneck, H., Stahlschmidt, S., Fehr, J. (2021) Finite Element Simulations of Motorcyclist Interaction with a Novel Passive Safety Concept for Motorcycles. *Proceedings of IRCOBI Conference*, 2021, Munich, Germany.

[15] Maier, S., Helbig, M., Hertneck, H., Fehr, J. (2021) Characterisation of an Energy Absorbing Foam for Motorcycle Rider Protection in LS-DYNA. *Proceedings of the 13th European LS-DYNA Conference*, 2021, Ulm, Germany.

[16] Gayzik, F., Moreno, D. *et al.* (2012) Development of a Full Human Body Finite Element Model for Blunt Injury Prediction Utilizing a Multi-Modality Medical Imaging Protocol. *Proceedings of the 12th International LS-DYNA Users Conference,* 2012*,* Dearborn, MI, USA.

[17] Iwamoto, M., Nakahira, Y. (2015) Development and Validation of the Total HUman Model for Safety (THUMS) Version 5 Containing Multiple 1D Muscles for Estimating Occupant Motions with Muscle Activation During Side Impacts. *Proceedings of the 59th Stapp Car Crash Conference*, 2015, New Orleans, LA, USA.

[18] OpenVT, https://openvt.eu/fem/viva/vivaplus_v0_2/. [2021-23-09]

[19] Schubert, A.; Erlinger, N.; Leo, C.; Iraeus, J.; John, J.; Klug, C. (2021) Development of a 50th Percentile Female Femur Model. *Proceedings of IRCOBI Conference*, 2021, Munich, Germany.

[20] John, J., Klug, C., Kranjec M., Svenning, E., Iraeus, J. (2022) Hello, World! VIVA+: A Human Body Model lineup to evaluate Sex-Differences in Crash Protection. *OSF Preprints,* April 29 2020. doi:10.31219/osf.io/uvkjc.

[21] Kolling, J. (1997) Validierung und Weiterentwicklung eines CAD-Menschmodells für die Fahrzeuggestaltung. 1997, Munich, Germany. (in German)

[22] PIPER Project, https://www.project-piper.io/. [2022-18-03]

[23] Zellner, J.W., Wiley, K.D. *et al.* (1996) A Standardized Motorcyclist Impact Dummy for Protective Device Research. *Proceedings of the 15th International Technical Conference on the Enhanced Safety of Vehicles (ESV)*, 1996, Melbourne, Australia.

[24] ISO 13232:2005 (2005) Motorcycles – Test and analysis procedures for research evaluation of rider crash protective devices fitted to motorcycles.

[25] Schmitt, K.-U., Niederer, P.F., Cronin, D.S., Morrison III, B., Muser, M.H., Walz, F. (2019) *Trauma Biomechanics*: *An Introduction to Injury Biomechanics*, Springer, Cham, Switzerland.

[26] VIRTUAL project, https://www.projectvirtual.eu/. [2022-28-03]

VIII. APPENDIX

Appendix A: Calculation of injury criteria

TABLE A.I
HEAD INJURY CRITERIA USED IN THIS STUDY AND RESPECTIVE BIOMECHANICAL LIMITS [25]

criterion	calculation	limit
Head Injury Criterion (36 ms)	$\mathrm{HIC(36)} = \max_{t_1,t_2}\left\{(t_2-t_1)\left[\frac{1}{t_2-t_1}\int_{t_1}^{t_2} a(t)dt\right]^{2.5}\right\}$ with $a(t)$ in g, t in s, and $t_2 - t_1 \leq 36$ ms	1000
resultant head acceleration	$\mathrm{a_{3ms}} = \max_{t_1}\left(\min_{t_1 \leq t \leq t_1+3\mathrm{ms}} a(t)\right)$	80 g
Generalized Acceleration Model for Brain Injury Threshold	$\mathrm{GAMBIT} = \left[\left(\frac{a_{\mathrm{res}}(t)}{250}\right)^{2.5} + \left(\frac{\ddot{\varphi}_{\mathrm{res}}(t)}{25}\right)^{2.5}\right]^{\frac{1}{2.5}}$ with $a_{\mathrm{res}}(t)$ in g and $\ddot{\varphi}_{\mathrm{res}}(t)$ in krad/s^2	1
Brain Injury Criterion	$\mathrm{BrIC(CMSD)} = \sqrt{\left(\frac{\max\lvert\omega_x\rvert}{\omega_{xC}}\right)^2 + \left(\frac{\max\lvert\omega_y\rvert}{\omega_{yC}}\right)^2 + \left(\frac{\max\lvert\omega_z\rvert}{\omega_{zC}}\right)^2}$ with $\omega_{xC} = 66.2, \omega_{yC} = 59.1$ and $\omega_{yC} = 41.25$ rad/s	1

Appendix B: Impact kinematics of GHBMC M50 and THUMS AM50 in ISO-13232 configuration ⑦ and ①

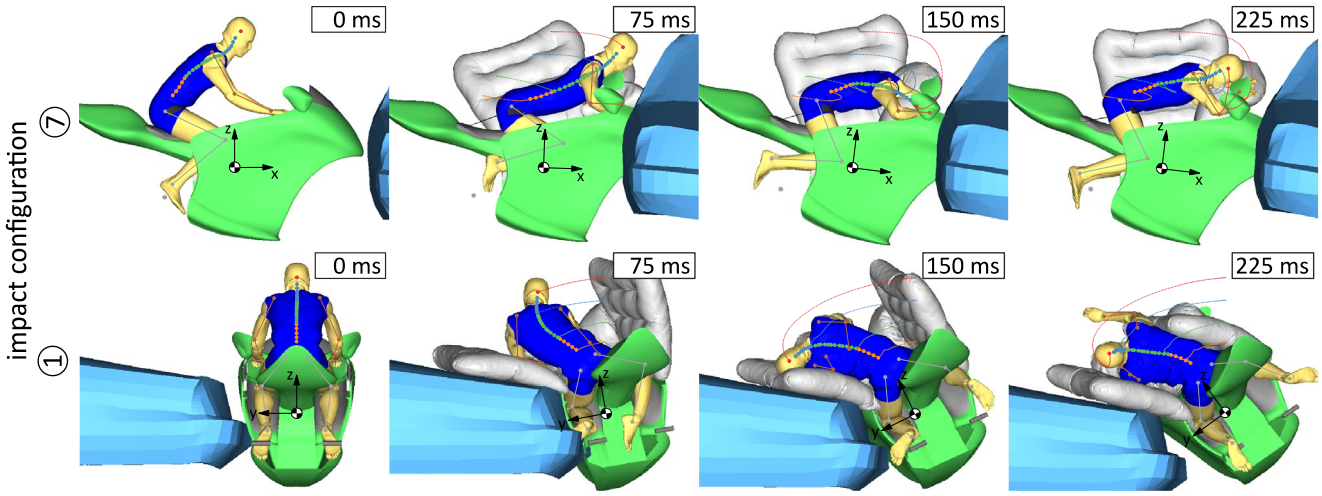

Fig. B.1. Impact simulations of GHBMC in ISO-13232 configuration ⑦ (top) and ① (bottom) with skeletal trajectories relative to the motorcycle's centre of gravity.

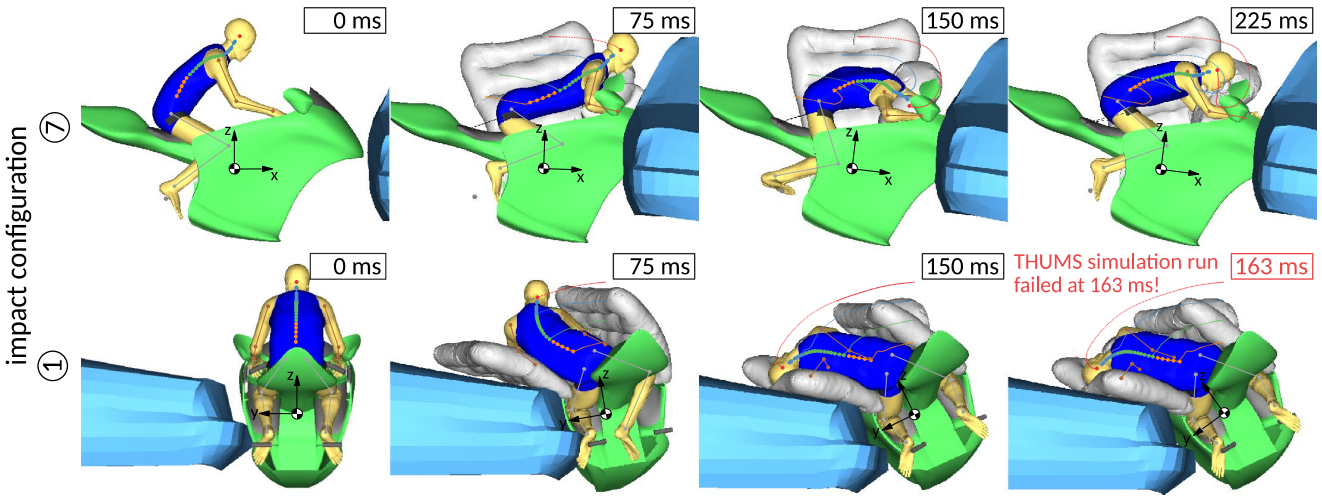

Fig. B.2. Impact simulations of THUMS in ISO-13232 configuration ⑦ (top) and ① (bottom) with skeletal trajectories relative to the motorcycle's centre of gravity. Note: the simulation of configuration ① failed at 163 ms!

Appendix C: Head COG angular velocities for Hybrid III 50th percentile, ViVA+ 50M, and GHBMC with determination of Brain Injury Criterion (BrIC)]

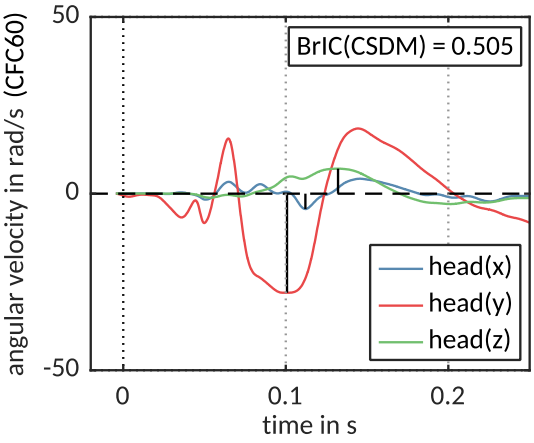

Fig. C.1. Head COG angular velocities of the Hybrid III 50th percentile in configuration ⑦.

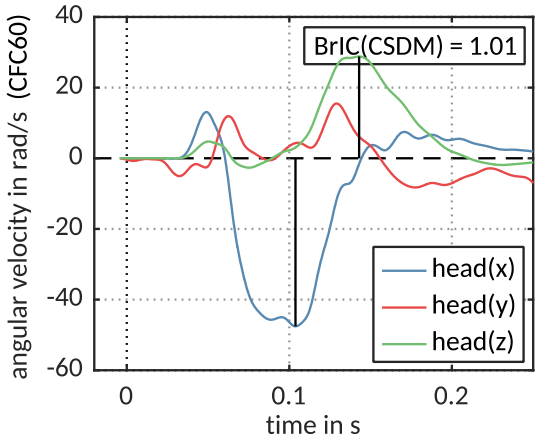

Fig. C.2. Head COG angular velocities of the Hybrid III 50th percentile in configuration ①.

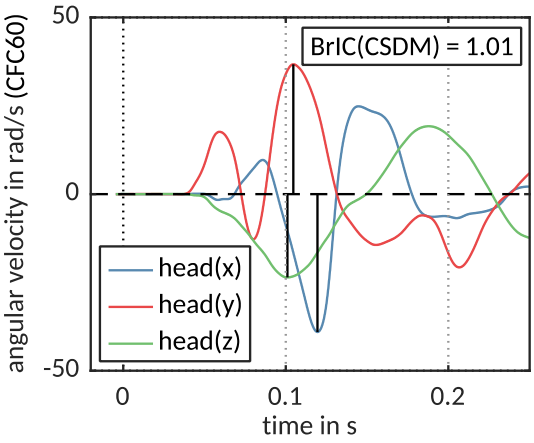

Fig. C.3. Head COG angular velocities of ViVA+ 50M in configuration ⑦.

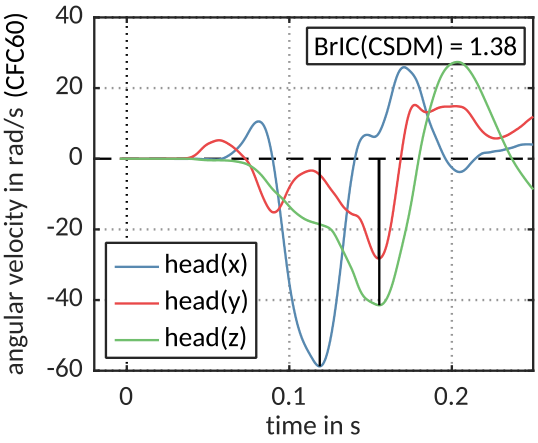

Fig. C.4. Head COG angular velocities of ViVA+ 50M in configuration ①.

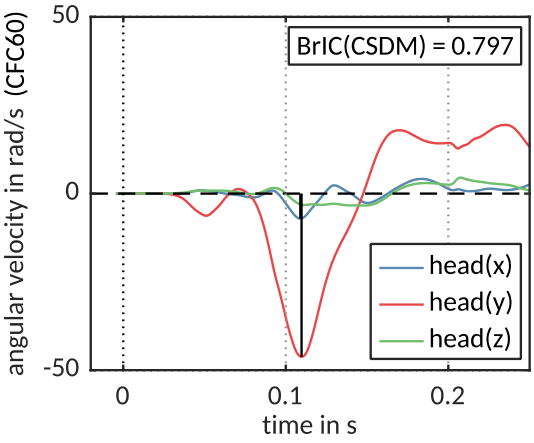

Fig. C.5. Head COG angular velocities of GHBMC in configuration ⑦.

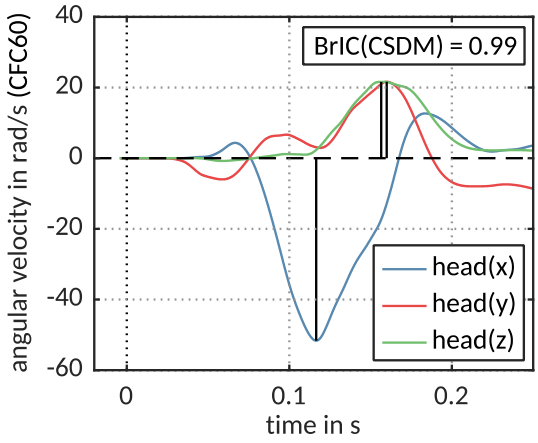

Fig. C.6. Head COG angular velocities of GHBMC in configuration ①.